



Published in final edited form as:

Ann Neurol. 2021 April ; 89(4): 726–739. doi:10.1002/ana.26015.

Tuber locations associated with infantile spasms map to a common brain network

Alexander L Cohen, MD, PhD^{1,3,9}, Brechtje PF Mulder, BSc^{1,2}, Anna K Prohl, BA³, Louis Soussand, MS⁹, Peter Davis, MD¹, Mallory R Kroeck, MA^{1,3,9}, Peter McManus, BA^{1,3,9}, Ali Gholipour, PhD³, Benoit Scherrer, PhD³, E. Martina Bebin, MD, MPA⁴, Joyce Y Wu, MD⁵, Hope Northrup, MD⁶, Darcy A Krueger, MD, PhD⁷, Mustafa Sahin, MD, PhD^{1,8}, Simon K Warfield, PhD³, Michael Fox, MD, PhD^{*,9,10,11}, Jurriaan M Peters, MD, PhD^{*,1,3} TACERN study group.

¹Department of Neurology, Boston Children's Hospital, Harvard Medical School, Boston, MA, USA ²VUmc School of Medical Sciences, Amsterdam UMC location VUmc, Amsterdam, The Netherlands ³Computational Radiology Laboratory, Department of Radiology, Boston Children's Hospital, Harvard Medical School, Boston, MA, USA ⁴Department of Neurology, University of Alabama at Birmingham, Birmingham, AL, USA ⁵Division of Pediatric Neurology, UCLA Mattel Children's Hospital, David Geffen School of Medicine, University of California Los Angeles, Los Angeles, CA ⁶Division of Medical Genetics, McGovern Medical School, The University of Texas Health Science Center at Houston, Houston, TX ⁷Department of Neurology, Cincinnati Children's Hospital Medical Center, Cincinnati, Ohio, USA ⁸F.M. Kirby Neurobiology Center, Boston Children's Hospital, Harvard Medical School, Harvard University, Boston, Massachusetts, USA. ⁹Laboratory for Brain Network Imaging and Modulation, Berenson-Allen Center for Non-Invasive Brain Stimulation and Division of Cognitive Neurology, Department of Neurology, Beth Israel Deaconess Medical Center, Harvard Medical School, Boston, MA, USA ¹⁰Athinoula A. Martinos Centre for Biomedical Imaging, Department of Radiology, Massachusetts General Hospital, Charlestown, MA, USA ¹¹Department of Neurology, Massachusetts General Hospital, Harvard Medical School, Boston, MA, USA

Abstract

Objective: Approximately 50% of patients with Tuberous Sclerosis Complex develop infantile spasms, a sudden-onset epilepsy syndrome associated with poor neurological outcomes. While an

Corresponding Author Information: Alexander Li Cohen, MD, PhD, Department of Neurology, Boston Children's Hospital, 300 Longwood Avenue, Boston, MA 02115, alexander.cohen2@childrens.harvard.edu, phone: 617-355-2069, fax: 617-730-0288.

*denotes co-senior authorship

Author Contributions

AC, BM, MF, MS, DK, JW, MB, HN, SW, and JP contributed to the conception and design of the study; AC, BM, MF, MS, DK, JW, MB, HN, AP, LS, PD, AG, MK, PM, BS, SW, and JP contributed to the acquisition and analysis of data; AC, BM, MF, and JP contributed to drafting a significant portion of the text and preparing the figures. Members of the TACERN group that contributed data for this project are listed in the supplementary online table.

Publisher's Disclaimer: This article has been accepted for publication and undergone full peer review but has not been through the copyediting, typesetting, pagination and proofreading process which may lead to differences between this version and the Version of Record. Please cite this article as doi: [10.1002/ana.26015](https://doi.org/10.1002/ana.26015)

Potential Conflicts of interest
Nothing to report.

increased burden of tubers confers an elevated risk of infantile spasms, it remains unknown whether some tuber locations confer higher risk than others. Here, we test whether tuber location and connectivity are associated with infantile spasms.

Methods: We segmented tubers from 123 children with (n=74) and without (n=49) infantile spasms from a prospective observational cohort. We used voxel-wise lesion symptom mapping to test for an association between spasms and tuber location. We then used lesion network mapping to test for an association between spasms and connectivity with tuber locations. Finally, we tested the discriminability of identified associations with logistic regression and cross validation as well as statistical mediation.

Results: Tuber locations associated with infantile spasms were heterogeneous, and no single location was significantly associated with spasms. However, >95% of tuber locations associated with spasms were functionally connected to the globus pallidi and cerebellar vermis. These connections were specific compared to tubers in patients without spasms. Logistic regression found that globus pallidus connectivity was a stronger predictor of spasms (OR 1.96, 95% CI [1.10, 3.50], p=0.02) than tuber burden (OR 1.65, 95% CI [0.90, 3.04], p=0.11), with a mean ROC area under the curve of 0.73 (+/-0.1) during repeated cross validation.

Interpretation: Connectivity between tuber locations and the bilateral globus pallidus is associated with infantile spasms. Our findings lend insight into spasm pathophysiology and may identify patients at risk.

Introduction

Tuberous Sclerosis Complex (TSC) is a neurogenetic disorder with an incidence of 1 in 6,000 live births¹ resulting from pathogenic variants in either the *TSC1* or *TSC2* genes. TSC is characterized by overactivation of the mechanistic target of rapamycin (mTOR) pathway leading to abnormalities in cell growth, differentiation, and migration which cause the formation of macroscopic lesions in the brain, including tubers, radial migration lines, and subependymal nodules. In particular, tubers demonstrate aberrant cortical lamination and contain poorly differentiated cells with an ambiguous neuronal-glial phenotype akin to focal cortical dysplasia type IIb². Tubers are potentially epileptogenic and in cases of refractory epilepsy in TSC patients, often represent the target of epilepsy surgery³.

Approximately 50% of children with TSC develop infantile spasms, a rapid-onset early childhood epilepsy syndrome which typically occurs in the first year of life as clusters of generalized flexor or extensor spasms^{4,5}, and can occur with numerous structural, metabolic, and genetic etiologies⁶. Since tubers are thought to disrupt local cortical architecture, others have studied whether tuber distribution can predict specific neurological phenotypes, including infantile spasms⁷⁻⁹. Unfortunately, these associations have not been consistently replicated across cohorts¹⁰⁻¹². A recent study of *non-TSC related* infantile spasms found that early acquired brain injury to deep grey matter nuclei may be associated with an increased risk for infantile spasms¹³; however, a consistent and reproducible pattern of lesion locations that leads to infantile spasms has not yet been found^{8,9,14}. Furthermore, the pathophysiology of how focal lesions result in generalized epileptic spasms remains unknown¹³. As such,

there is a knowledge gap in understanding whether specific patterns of cerebral involvement are associated with infantile spasms.

One approach to linking lesion location and symptom expression is voxel-wise lesion symptom mapping, typically used to study clinical syndromes in acute stroke¹⁵. When lesion locations across patients with similar symptoms overlap, neurological symptoms can be attributed to specific brain regions. While tuber burden and qualitative tuber location have been examined, formal voxel-wise lesion symptom mapping of tubers for specific symptoms in TSC has not yet been explored, likely due to the need for larger sample sizes and computer-aided lesion delineation^{8,9,14}.

It is possible, however, that infantile spasms result from injury to a specific *network*, as opposed to dysfunction of a single region. Lesion network mapping identifies the network of brain regions *connected* to each lesion location using a normative map of functional connectivity¹⁶. Connections associated with a specific symptom can then be identified. This technique has been successfully used to elucidate lesion-induced hallucinations, delusions, movement disorders, and a variety of other symptoms¹⁶⁻²⁰, and lesion network mapping results have shown promise as treatment targets for therapeutic brain stimulation²¹. Here, we identified tuber distributions from a large cohort of patients with TSC and applied both traditional voxel-wise lesion symptom mapping and more novel lesion network mapping to determine whether there is a spasmogenic network that is critical to the generation of infantile spasms.

Methods

Patients

Patients's data were obtained from the Tuberous Sclerosis Complex Autism Center of Excellence Network's (TACERN) multi-center prospective study (NIH U01 NS082320)⁴. Patients were enrolled in the first year of life and followed longitudinally through 36 months of age. Informed consent was obtained for each patient, as approved by the Institutional Review Board at each participating site. Inclusion criteria for the current study included availability of high-quality structural neuroimaging demonstrating visibly present cortical tubers.

Tuber segmentation and co-registration

Each patient's T1w structural MRI was processed as previously described². As tubers show minimal evolution in location and volume on imaging², the highest contrast MRI (at age >2 years old) was used. An automated lesion segmentation algorithm²² was trained on 20 manually segmented T1w, T2w and FLAIR MRI images of children with TSC and validated on images from an additional ten children, all of whom were not patients in the present study. This algorithm was then applied to each patient's neuroimaging, followed by visual inspection and manual correction of all tuber segmentations with ITK-SNAP²³. In all cases, the final delineation of tuber distributions was subject to experienced expert review (JP). All identified tuber voxels for each participant were coded equally, i.e., not segmented into separable tubers. We then registered each patient's tuber distribution to a common space

using the MNI152 2009c nonlinear asymmetric template and Advanced Normalization Tools (ANTs) software, which allows ‘unweighting’ of lesion locations²⁴.

Voxel-wise lesion symptom mapping of tuber distributions associated with infantile spasms

We performed voxel-wise lesion symptom mapping to identify relationships between specific tuber location and infantile spasms^{15,25}. At each voxel affected by at least three tubers across the 123 patients²⁶, the association of tuber presence and infantile spasms was tested via Liebermeister test, using permutation-based voxel-wise statistics controlling for family-wise error with NiiStat²⁵. To account for the spatial dependence between adjacent voxels, a whole-brain Bayesian Spatial Generalized Linear Mixed Model (BSGLMM)²⁷ was used to determine the probability of tuber presence in patients with and without infantile spasms.

Quantitative assessment of overall tuber location and burden

Lobar and overall cortical grey matter burden were calculated using masks created from the MNI probabilistic structural atlas distributed with FSL²⁸ (thresholded at 15). A 2-way ANOVA assessed for main effect of group, main effect of lobe, and for group x lobe interaction (www.R-project.org). To compare with prior work assessing the presence or absence of tubers in particular lobes, we also calculated the percentage of patients with lobar involvement > 0.5%, omitting lobes with minimal tuber pathology.

Lesion network mapping of tuber distributions associated with infantile spasms

The tuber segmentation from each patient with infantile spasms was used as a seed in a resting-state functional connectivity analysis of data collected from 1,000 healthy young-adult controls²⁹, similar to prior studies¹⁶⁻²¹, creating a T map for each patient where the value of each voxel represents the functional connectivity between that voxel and segmented tubers. Each patient’s T map was then thresholded ($T > \pm 11$, voxel-wise FWE corrected at $P < 10^{-12}$) to create a binarized map of regions strongly functionally connected to each patient’s tuber distribution. The overlap of these maps identified voxels consistently functionally connected to tubers. A clustering algorithm (Nilearn connected_regions³⁰) was used to identify regions of interest (ROIs) of $> 50\text{mm}^3$ that were $> 95\%$ sensitive for infantile spasms. To maximize the spatial specificity of our localization, a threshold of $T > \pm 11$ was utilized; using thresholds of $T > \pm 9$ or 7 did not change the interpretation of our results³¹, and all statistical analyses described below used continuous values which did not depend on a threshold/cutoff.

Split-half replication of lesion network mapping results

To assess the reliability of our lesion network overlap results, we divided our infantile spasms cohort into two subsets of 37 patients each. We then repeated the above lesion network mapping on each subset and connected regions derived using the same T-score threshold as above. As such, this represented a test of the sensitivity of the overlap procedure across patients with infantile spasms.

Specificity of tuber distribution connectivity for infantile spasms

We also assessed the specificity of functional connectivity patterns for infantile spasms as in prior lesion network mapping studies¹⁶⁻²¹. A voxel-wise two-sample t-test was performed via permutation testing (FSL PALM v.alpha109) using 2000 permutations, tail approximation²⁵, and a voxel-wise family-wise error rate corrected $p < 0.05$. Permutation testing and voxel-wise statistics were chosen because they are more resilient to false-positives seen with cluster-based approaches³².

Identifying connections and tuber locations both sensitive and specific to TSC associated infantile spasms

We next identified regions that were *both* sensitive and specific for infantile spasms, i.e., the conjunction of voxels functionally connected to 95% of tuber distributions causing infantile spasms and demonstrating statistically stronger connectivity to tubers in patients with infantile spasms vs. without. We also used these regions as functional connectivity seeds to perform an inverse mapping, i.e., defining the brain network that best encompasses tubers uniquely associated with infantile spasms. While circular, this allows for visual inspection of which individual tuber or set of tubers in any given patient may be most likely driving the association with infantile spasms.

Replication of lesion network mapping results across genetic diagnoses

Since TSC2 gene mutation is often associated with a more severe phenotype, we tested whether the patterns seen in the overall cohort depended on genetic diagnosis by repeating the above permutation-based two-sample t-test with genetic diagnosis included as a covariate and by performing both the lesion network overlap and statistical testing separately in genetically consistent subsamples. For the latter, we generated a cohort of 76 patients with confirmed TSC2 gene mutations (47 with infantile spasms) and a cohort of the remaining 47 patients with either TSC1 gene mutations or indeterminate gene mutations (27 with infantile spasms).

Replication of lesion network mapping results with pediatric functional connectome data

To assess the consistency of our findings with pediatric connectivity data, we repeated the analyses above using data from the Adolescent Brain Cognitive Development (ABCD) study of 10,000 9-10 year-old participants which recently became available NIMH Data Archive Collection #3165 (https://nda.nih.gov/edit_collection.html?id=3165)³³. This represents the 'youngest' large-scale normative functional connectivity data currently available. A cohort of 1000 participants were identified with parameters consistent with our young adult connectome³¹, i.e., acquired on Siemens MRI scanners, without reported DSM-5 criteria diagnoses or TBI, and with low in-scanner movement. The latter was approximated via the number of BOLD timepoints below a framewise displacement (FD) threshold of 0.2. Preprocessing of this ABCD cohort was performed using FreeSurfer7.1³⁴ and a modified version of the Computational Brain Imaging Group (CBIG) functional connectivity preprocessing pipeline³⁵ (<https://github.com/bchcohenlab>) that more closely reflects the preprocessing of the original young adult cohort³⁶. Lesion network mapping and specificity analyses were then performed as described above. Due to differences in statistical power of

the connectivity patterns seen in the ABCD dataset with the current processing pipeline, a T threshold of $T > \pm 9$ (voxel-wise FWE corrected at $P < 10^{-12}$) appeared to be most similar to a $T > \pm 11$ in the young adult connectome.

Identifying independent predictors of infantile spasms with logistic regression

We modeled the binary outcome of infantile spasms using logistic regression using the Statsmodels python package³⁷. The models related infantile spasms to the independent variables of tuber-to-identified ROI correlations and tuber burden for our 123 patients. Odds ratios, 95% confidence intervals, McFadden pseudo R^2 , and Akaike Information Criterion (AIC) were then computed.

Consistency testing via Repeated Stratified K-fold cross validation

We used cross validation to test the internal reproducibility of predicting infantile spasms based on our findings. Using the logistic regression model that best described the data, we performed a Repeated Stratified K-Fold cross validation using Scikit-learn³⁸, iteratively training a model using 80% of the 123 patients, maintaining the relative ratio of patients with and without spasms. This model was then used to classify the remaining 20%. The classification results of 5,000 iterations, with random shuffling within groups, was used to create Receiver Operating Characteristic curves. We then calculated the mean area under the curve and the variance of the curve when differing subsets of the data are used. Distinct from the split half replication above, this analysis tests the consistency of the difference between patients with and without infantile spasms.

Assessing for mediation of the relationships between independent predictors and infantile spasms

Finally, we performed a statistical mediation analysis³⁹ using the SPSS PROCESS macro⁴⁰ to determine whether the identified relationship between independent predictors and infantile spasms were a by-product of statistical mediation. In other words, does X predict Y ($X \rightarrow Y$) solely or in part because X predicts M, which in turn predicts Y ($X \rightarrow M \rightarrow Y$). Reverse models were also assessed to be agnostic in regard to the directionality of mediation. 5000 bootstrap samples were used to calculate significance of the indirect pathway via confidence intervals.

Results

Patient demographics

We identified 142 children that completed all study visits with clinical and/or genetic criteria for definite TSC from the prospective multicenter TACERN dataset⁴. Nineteen patients were excluded due to either a lack of available neuroimaging ($n=1$), or a lack of visibly present tubers present on neuroimaging ($n=18$, three of whom had infantile spasms). During study follow-up through 3 years of age, 74 patients developed infantile spasms, while 49 patients did not (Figure 1). The two groups were largely similar in regard to sex (47% male vs. 57%) and age at time of neuroimaging (2.74 vs. 2.53 years old). We found a higher prevalence of infantile spasms in patients with a *TSC2* gene mutation compared to those with a *TSC1* gene mutation (67% vs. 21%, $p=0.012$), consistent with prior work⁴ (Table 1). As expected, all

patients that developed infantile spasms received antiepileptic agents *after* the development of spasms, consistent with standard recommendations. Of note, 13 patients who developed infantile spasms (17.6%) received antiepileptic medications *prior* to the onset of infantile spasms to treat other semiologies. Of these, only levetiracetam (n=9) was used in more than 3 patients. Conversely, 28 patients (57.1%) who did not develop infantile spasms received antiepileptic medications for other semiologies. If this treatment prevented the development of infantile spasms in a proportion of patients, this would have created bias against the findings presented below and thus does not represent a limitation.

Distribution of tubers in TSC

The number and spatial location of tubers was highly heterogeneous across patients (Figure 2). The median tuber burden for our entire cohort was 2.10% of the cortical grey matter (24.7 cm³) (Table 1). Tubers were largely stochastically distributed across the brain (Figure 3A). While visual inspection suggested a relative sparing of primary motor and visual cortices, this pattern was not statistically significant when assessed using *a priori* parcellations, nor did this differentiate between patients with and without infantile spasms (Figure 3B and 3C).

Association of tuber locations with a history of infantile spasms

No single brain region was affected by tubers in all cases of infantile spasms. In fact, the maximum overlap of tuber locations across the cohort with spasms was only 24.3% (18/74 patients). Voxel-wise lesion symptom mapping failed to identify any significant associations between tuber location and infantile spasms, and the highest predictive value of any location for infantile spasms was 24% (Figure 3D). Although overall tuber burden was higher in patients with infantile spasms than in those without (two-way ANOVA 2.59% vs. 0.85%, $p < .0001$), there was no significant difference across different brain lobes ($p = 0.144$) (Figure 3E and F, Table 1).

Lesion network mapping of tubers in TSC patients with infantile spasms

The network of brain regions functionally connected to each patient's tuber locations was computed (Figure 4A-B), and connections common to >95% of the 74 patients with infantile spasms were identified (Figure 4C). Both left and right internal segments of the globus pallidus and the cerebellar vermis (lobule VIIIA) demonstrated consistent negative functional connectivity with tuber distributions associated with infantile spasms. Peak voxel-wise overlap was 72/74 patients in the right globus pallidus, 73/74 in the left globus pallidus, and 74/74 in the cerebellar vermis. Split-half replication demonstrated consistent localization of this overlap across independent subgroups (Figure 4D). Repeating this analysis solely for patients with TSC2 mutations (n=47) and solely for patients with either confirmed TSC1 or indeterminate mutations (n=27) both also identified consistent localization to the bilateral globus pallidus and cerebellar vermis. Performing lesion network mapping on the tuber distributions from the 49 children without infantile spasms did not reveal any consistently connected regions.

Specificity of lesion network connectivity patterns for infantile spasms

A vowel-wise permutation-based two-sample t-test was used to compare lesion network maps of patients with versus without infantile spasms, controlling for genetic diagnosis as a covariate. Negative connectivity to the bilateral globus pallidus and cerebellar vermis was highly specific to patients with versus without infantile spasms (FWE corrected $p < 0.05$) and was not driven by the higher incidence of infantile spasms among patients with TSC2 gene mutations noted above⁴. The conjunction of a mask of these significant voxels and the lesion network mapping analysis above generated a map of regions both sensitive and specific for infantile spasms (Figure 4E).

Replication of lesion mapping results with pediatric functional connectome data

Repeating the above analyses using a pediatric normative connective (1000 9-year-old participants from the ABCD Study) identified consistent connectivity patterns. Regions were again identified in the left and right globus pallidus, with peak voxel-wise overlap of 63/74 in each, and 65/74 in the cerebellar vermis. A two-sample t-test was again computed as above, and the intersection of these regions with a mask of significant voxels (uncorrected $p < 0.005$) was again computed to identify regions both sensitive and specific for infantile spasms (Figure 4F).

Tuber locations most likely to be associated with infantile spasms

A map was created from the intersection of regions with both strong negative connectivity to the globus pallidus and strong negative connectivity to the cerebellar vermis (Figure 5A). This defined a specific brain network that best encompasses tuber locations associated with infantile spasms. Comparison of the tuber distributions from patients with and without infantile spasms (Figure 5B-C) demonstrates a higher proportion of tuber-network overlap in patients with infantile spasms (Figure 5B, **blue circles**), even in patients with low tuber burden, e.g., Participant L1 vs Participant L2.

Evaluating independent predictors of infantile spasms

Tuber burden, globus pallidus connectivity, and cerebellar vermis connectivity were each separately associated with infantile spasms (Table 2, **Models 1, 2, and 3**). However, in combined models that included connectivity to the globus pallidus, all other independent variables became non-significant (Table 2, **Models 4, 5, and 6**). A model relating tuber burden and globus pallidus connectivity best represented the underlying data and explained the most variance (Table 2, **Model 5**). In this model, globus pallidus connectivity was a stronger predictor of infantile spasms than tuber burden (OR 1.96, 95%CI [1.10, 3.50], $p = 0.02$ vs. OR 1.65, 95%CI [0.90, 3.04], $p = 0.18$). Repeated stratified K-fold cross validation of this model, using 80% of the 123 patients to train and testing for accuracy with the remaining 20%, was moderately accurate across 5,000 iterations, with a mean Receiver Operating Characteristic Area Under the Curve of 0.73 (SD=0.10) (Figure 6A).

Assessing for mediation of the relationships between tuber burden, globus pallidus connectivity, and infantile spasms

A statistical mediation analysis found that the relationship between connectivity to the globus pallidus and infantile spasms was not the by-product of increased tuber burden, i.e., no mediation was detected (indirect effect: $ab=-0.306$, boot SE=0.2091, 95% CI (-0.786,0.046). However, the reverse model (Figure 6B) found that the relationship between tuber burden and infantile spasms (*path c*) was fully mediated by connectivity to the globus pallidus, i.e., increased tuber burden predicts (*path a*) increased connectivity to the globus pallidus, which in turn predicts (*path b*) infantile spasms (indirect effect: $ab=0.412$, boot SE=0.194, 95% CI (0.114,0.872). When this mediation is taken into account, tuber burden was no longer an independent predictor (*path c'*) of infantile spasms consistent with our logistic regression results (Table 2).

Discussion

In this large, prospectively acquired and highly characterized TSC cohort derived from the TACERN study, we quantified the impact of tuber burden, location, and network involvement on infantile spasms. In line with previously described cohorts, tuber burden was higher in patients with infantile spasms^{14,41,42}, likely reflecting a more severe disease burden^{12,14,43}, however our results suggest a possible mechanism for this observation.

We found that neither tuber burden within particular lobes nor at specific locations across the brain were associated with infantile spasms. Instead, the distribution of tubers in children with infantile spasms defines a specific set of brain regions that is characterized by strong negative connectivity to the bilateral globus pallidus and cerebellar vermis. This finding was highly sensitive and specific to infantile spasms, was consistent across split half replication, genetic etiology, medication exposure, using a pediatric connectome to derive normative connectivity patterns, and demonstrated a stronger independent association with infantile spasms than tuber burden did alone.

These findings have two implications. First, network connectivity may explain why some children develop infantile spasms, and others do not, through the convergence of anatomically variable lesions on a common pathway. This may also explain why increased tuber burden is also associated with spasms, as more tubers increase the likelihood that the identified network of brain regions is affected. Our mediation analysis suggests that increased connectivity between tuber locations and the globus pallidus may mediate the known association between tuber burden and infantile spasms; however, since the identification of globus pallidus connectivity as a predictor was also generated from this same dataset, hypothesis testing in this direction should be done with caution. Although there is increased excitability on a cellular level in TSC and increased epileptogenicity in brain tissue at and surrounding tubers, the basis of why infantile spasms are so prevalent in TSC, compared to other etiologies, is unknown⁴⁴. Study of other lesional causes of infantile spasms, including early life stroke and periventricular leukomalacia, is needed to test whether the identified nodes in this pathway are consistent across causes of infantile spasms⁶, or whether they are unique to TSC.

Second, while more speculative, these findings lend further support to a proposed role for cortical-subcortical network interactions in the pathophysiology of infantile spasms⁴⁵. Several converging lines of evidence suggest that the basal ganglia are a central “hub” in a spasmogenic network affected by focal cortical lesions. Specifically, generalized epileptic spasms can resolve by surgical resection of singular focal structural lesions⁴⁶; patients with congenital or early structural lesions that encompass the basal ganglia are at an increased risk for infantile spasms¹³; and both PET and EEG-fMRI studies of infantile spasms have demonstrated extension of the epileptic network to the lenticular nuclei^{47,48}.

Our results implicate the globus pallidus in the pathophysiology of infantile spasms, but the exact mechanism - and whether the globus pallidus may represent a therapeutic target - remains unknown. There is evidence that globus pallidus inhibition can lead to seizures in some scenarios but can lead to improved seizure control in others⁴⁹. While less is known about the role of the cerebellar vermis in epilepsy, it is involved in the cortico-reticulo-cerebellar pathway to support movement generation and projects to the deep cerebellar nuclei, which have a hub-like function for all output of the cerebellar network and an additional role in GABAergic inhibition⁵⁰. Furthermore, one of the most effective therapies for infantile spasms, vigabatrin, is an irreversible inhibitor of GABA aminotransferase, and while effective, can also lead to cytotoxic edema in the brainstem, dentate nuclei of the cerebellum, thalamus, and globus pallidus, consistent with their role in GABAergic metabolism and prominent concentration of GABAergic neurons⁵¹⁻⁵³. Conversely, rodent models of infantile spasms often require simultaneous injury to both cortical and subcortical structures including the thalamus and striatum⁵⁴. We speculate that dysfunction of the globus pallidus or cerebellar vermis alone is not sufficient to generate spasms and that increased cortical activity, in combination with failure of the modulating effects from these subcortical structures, culminates in infantile spasms⁴⁵.

The finding that tuber locations are negatively correlated with the globus pallidus in children with infantile spasms means that as the fMRI signal at tuber locations goes up, the fMRI signal in the globus pallidus and cerebellar vermis goes down, and vice-versa. However, the physiological interpretation of negative correlations, as well as the directionality of the interactions seen in fcMRI data remain unclear⁵⁵. Tubers could act as spike generators, increasing local activity that leads to suppression of the globus pallidus and vermis. Conversely, tubers could act as lesions, decreasing local activity, leading to increased activity in the connected structure. Alternatively, activity in the globus pallidus or vermis could influence cortical excitability at tuber locations. Future work is needed to better understand the link between tuber locations associated with infantile spasms, the globus pallidus, and the vermis.

Limitations

First, we have primarily used a normative young adult group connectome (n=1000, ages 18-35) to study the connectivity patterns for lesion network mapping³¹. This provides significant signal-to-noise advantages, allows for technique standardization, and has been highly informative¹⁶⁻²¹. While this does provide a true indication of the developmental *endpoints* of connectivity between brain regions, it ignores age-related differences in

connectivity that may be important here. However, a large high-quality functional connectivity dataset from ~2-3-year-old children is not currently available; and a direct test of lesion network mapping using an age-matched connectome is not yet feasible. Nevertheless, we have thus far seen minimal impact from methodological differences in how one processes connectome data, e.g. global signal regression versus other artifact removal strategies^{16,55}, or using patient-specific, age-, or disease-matched normative connectomes⁵⁶⁻⁶⁰; which is reflected here by the consistent localization of infantile spasms-related connections using data from the ABCD 9-year-old group connectome (n=1000), (Figure 4E vs Figure 4F). It is possible that our results could be improved by using a connectome better matched to the age of the TSC patients, and this is an experiment we intend to perform once such data becomes available and extensively processed given the significant confounds present in young child fMRI data.

Second, lesion network mapping has primarily been used to study lesion-induced disorders in previously healthy participants²⁰; however, tubers are congenital, affecting the maturation of developing brain networks⁶¹. We argue, however, that disruption of the local architecture drives the (partial) transfer of functions originally destined to be in those affected areas and that the dysplastic neurons in tubers generate abnormal activity locally⁴⁶.

Finally, the goal of the present study was to test whether tuber distributions associated with spasms map to a common brain network, to define this network, and to assess the consistency of this network. Whether tuber distributions associated with spasms directly correlate with functional connectivity differences in these same children is a topic we intend to pursue⁶¹. It is impossible, however, to delineate which of this altered connectivity represents causation, compensation, or downstream effects from infantile spasms. Since the presence, location, and extent of cortical tubers is consistent before and after the onset of spasms, we believe the presented analysis is more likely to represent causal information.

Conclusions

In summary, our results provide evidence for the location of key network nodes for a potential infantile spasms network, but further work is needed to understand the specific pathophysiology at these locations. We propose that future efforts to clarify the role these structures play in spasmogenesis via pallidal and vermian GABAergic knockout models and depth electrode studies, as well as comparison of the results presented here with cortical tuber resection outcomes and EEG source localization will also clarify the clinical implications of the presented results. Furthermore, lesion network mapping of individual tuber lesions rather than lesion patterns in patients with available EEG data may identify spasmogenic tubers, leading to an approach for candidate selection for epilepsy surgery or non-invasive brain stimulation.

At present, we have a moderate predictive ability to identify those at elevated risk for infantile spasms in TSC. Looking forwards, refinement of this predictive model with the inclusion of serial EEG data and EEG connectivity metrics will likely enhance its performance^{62,63}. Additionally, preventative treatment of seizures with vigabatrin is currently being studied for TSC in Europe⁶⁴ and the US ([NCT02849457](#)). Specific prediction of spasms based on our imaging methods may allow for improved risk-

stratification and limit exposure to vigabatrin for pre-emptive treatment to those at higher risk.

Supplementary Material

Refer to Web version on PubMed Central for supplementary material.

Acknowledgements

We are sincerely indebted to the generosity of the families and patients in TSC clinics across the United States who contributed their time and effort to this study. We would also like to thank the Tuberous Sclerosis Alliance for their continued support in TSC research.

GSP acknowledgement

Data were provided [in part] by the Brain Genomics Superstruct Project of Harvard University and the Massachusetts General Hospital, (Principal Investigators: Randy Buckner, Joshua Roffman, and Jordan Smoller), with support from the Center for Brain Science Neuroinformatics Research Group, the Athinoula A. Martinos Center for Biomedical Imaging, and the Center for Human Genetic Research. 20 individual investigators at Harvard and MGH generously contributed data to the overall project.

ABCD acknowledgement

Some of the data used in the preparation of this article were obtained from the Adolescent Brain Cognitive Development (ABCD) Study (<https://abcdstudy.org>), held in the NIMH Data Archive (NDA). This is a multisite, longitudinal study designed to recruit more than 10,000 children age 9-10 and follow them over 10 years into early adulthood. The ABCD Study is supported by the National Institutes of Health and additional federal partners under award numbers U01DA041022, U01DA041028, U01DA041048, U01DA041089, U01DA041106, U01DA041117, U01DA041120, U01DA041134, U01DA041148, U01DA041156, U01DA041174, U24DA041123, U24DA041147, U01DA041093, and U01DA041025. A full list of supporters is available at <https://abcdstudy.org/federal-partners.html>. A listing of participating sites and a complete listing of the study investigators can be found at <https://abcdstudy.org/scientists/workgroups/>. ABCD consortium investigators designed and implemented the study and/or provided data but did not necessarily participate in analysis or writing of this report. This manuscript reflects the views of the authors and may not reflect the opinions or views of the NIH or ABCD consortium investigators.

Funding:

This research was supported by awards from multiple NIH grants including the U01NS082320 (M.S. and D.K), T32MH112510 and K23MH120510 (A.C. and P.M.), U54NS092090 (M.S.), U54HD090255 (M.S.) and K23NS083741(M.F.) as well as funding from the TS Alliance to TACERN, the Child Neurology Foundation (A.C. and M.K.), the Sidney R. Baer, Jr. Foundation (M.F.), the Dystonia Foundation (M.F.), and the Nancy Lurie Marks Foundation (M.F.).

References

1. OSBORNE JP, FRYER A, WEBB D. Epidemiology of Tuberous Sclerosis. *Annals of the New York Academy of Sciences* 1991;615(1):125–127. [PubMed: 2039137]
2. Peters JM, Prohl AK, Tomas-Fernandez XK, et al. Tubers are neither static nor discrete. *Neurology* 2015;85(18):1536–1545. [PubMed: 26432846]
3. Liang S, Zhang J, Yang Z, et al. Long-term outcomes of epilepsy surgery in tuberous sclerosis complex. *Journal of Neurology* 2017;264(6):1146–1154. [PubMed: 28516327]
4. Davis PE, Filip-Dhima R, Sideridis G, et al. Presentation and diagnosis of tuberous sclerosis complex in infants. *Pediatrics* 2017;140(6):1–11.
5. Chu-Shore CJ, Major P, Camposano S, et al. The natural history of epilepsy in tuberous sclerosis complex. *Epilepsia* 2010;51(7):1236–1241. [PubMed: 20041940]
6. Osborne JP, Edwards SW, Dietrich Alber F, et al. The underlying etiology of infantile spasms (West syndrome): Information from the International Collaborative Infantile Spasms Study (ICISS). *Epilepsia* 2019;60(9):1861–1869. [PubMed: 31418851]

7. Bolton PF, Griffiths PD. Association of tuberous sclerosis of temporal lobes with autism and atypical autism. *Lancet* 1997;349(9049):392–395. [PubMed: 9033466]
8. Bolton PF, Park RJ, Higgins JNP, et al. Neuro-epileptic determinants of autism spectrum disorders in tuberous sclerosis complex. *Brain* 2002;125(6):1247–1255. [PubMed: 12023313]
9. Numis AL, Major P, Montenegro MA, et al. Identification of risk factors for autism spectrum disorders in tuberous sclerosis complex. *Neurology* 2011;76(11):981–987. [PubMed: 21403110]
10. Mous SE, Overwater IE, Vidal Gato R, et al. Cortical dysplasia and autistic trait severity in children with Tuberous Sclerosis Complex: a clinical epidemiological study. *European Child and Adolescent Psychiatry* 2018;27(6):753–765. [PubMed: 29063203]
11. Walz NC, Byars AW, Egelhoff JC, Franz DN. Supratentorial tuber location and autism in tuberous sclerosis complex. *Journal of Child Neurology* 2002;17(11):830–832. [PubMed: 12585723]
12. Ridler K, Suckling J, Higgins N, et al. Standardized whole brain mapping of tubers and subependymal nodules in tuberous sclerosis complex. *Journal of Child Neurology* 2004;19(9):658–665. [PubMed: 15563011]
13. Harini C, Sharda S, Bergin AM, et al. Detailed Magnetic Resonance Imaging (MRI) Analysis in Infantile Spasms. *Journal of Child Neurology* 2018;33(6):405–412. [PubMed: 29575949]
14. Jansen FE, Vincken KL, Algra A, et al. Cognitive impairment in tuberous sclerosis complex is a multifactorial condition. *Neurology* 2008;70(12):916–923. [PubMed: 18032744]
15. Rorden C, Karnath HO, Bonilha L. Improving lesion-symptom mapping. *Journal of Cognitive Neuroscience* 2007;19(7):1081–1088. [PubMed: 17583985]
16. Boes AD, Prasad S, Liu H, et al. Network localization of neurological symptoms from focal brain lesions. *Brain* 2015;138(10):3061–3075. [PubMed: 26264514]
17. Darby RR, Laganieri S, Pascual-Leone A, et al. Finding the imposter: Brain connectivity of lesions causing delusional misidentifications. *Brain* 2017;140(2):497–507. [PubMed: 28082298]
18. Darby RR, Horn A, Cushman F, Fox MD. Lesion network localization of criminal behavior. *Proceedings of the National Academy of Sciences of the United States of America* 2018;115(3):601–606. [PubMed: 29255017]
19. Cohen AL, Soussand L, Corrow SL, et al. Looking beyond the face area: Lesion network mapping of prosopagnosia. *Brain* 2019;142(12):3975–3990. [PubMed: 31740940]
20. Fox MD. Mapping symptoms to brain networks with the human connectome. *New England Journal of Medicine* 2018;379(23):2237–2245.
21. Joutsa J, Shih LC, Horn A, et al. Identifying therapeutic targets from spontaneous beneficial brain lesions. *Annals of Neurology* 2018;84(1):153–157. [PubMed: 30014594]
22. Hashemi SR, Salehi SSM, Erdogmus D, et al. Asymmetric Loss Functions and Deep Densely-Connected Networks for Highly-Imbalanced Medical Image Segmentation: Application to Multiple Sclerosis Lesion Detection. *IEEE Access* 2019;7:1721–1735.
23. Yushkevich P, Piven J, Cody H, Ho S. User-guided level set segmentation of anatomical structures with ITK-SNAP. *Neuroimage* 2006;31(3):1116–1128. [PubMed: 16545965]
24. Andersen SM, Rapcsak SZ, Beeson PM. Cost function masking during normalization of brains with focal lesions: Still a necessity? *NeuroImage* 2010;53(1):78–84. [PubMed: 20542122]
25. Winkler AM, Ridgway GR, Webster MA, et al. Permutation inference for the general linear model. *NeuroImage* 2014;92:381–397. [PubMed: 24530839]
26. Sperber C, Karnath HO. Impact of correction factors in human brain lesion-behavior inference. *Human Brain Mapping* 2017;38(3):1692–1701. [PubMed: 28045225]
27. Ge T, Müller-Lenke N, Bendfeldt K, et al. Analysis of multiple sclerosis lesions via spatially varying coefficients. *Annals of Applied Statistics* 2014;8(2):1095–1118.
28. Mazziotta J, Toga A, Evans A, et al. A probabilistic atlas and reference system for the human brain: International Consortium for Brain Mapping (ICBM). *Philosophical Transactions of the Royal Society B: Biological Sciences* 2001;356(1412):1293–1322.
29. Thomas Yeo BT, Krienen FM, Sepulcre J, et al. The organization of the human cerebral cortex estimated by intrinsic functional connectivity. *Journal of Neurophysiology* 2011;106(3):1125–1165. [PubMed: 21653723]

30. Abraham A, Pedregosa F, Eickenberg M, et al. Machine learning for neuroimaging with scikit-learn. *Frontiers in Neuroinformatics* 2014;8(FEB):14. [PubMed: 24600388]
31. Cohen AL, Fox MD. Reply: The influence of sample size and arbitrary statistical thresholds in lesion-network mapping. *Brain* 2020;143(5):e41–e41. [PubMed: 32365379]
32. Eklund A, Nichols TE, Knutsson H. Cluster failure: Why fMRI inferences for spatial extent have inflated false-positive rates. *Proceedings of the National Academy of Sciences of the United States of America* 2016;113(28):7900–7905. [PubMed: 27357684]
33. Volkow ND, Koob GF, Croyle RT, et al. The conception of the ABCD study: From substance use to a broad NIH collaboration. *Dev Cogn Neurosci* 2018;32:4–7. [PubMed: 29051027]
34. Fischl B *FreeSurfer*. *Neuroimage* 2012;62(2):774–781. [PubMed: 22248573]
35. Li J, Kong R, Liégeois R, et al. Global signal regression strengthens association between resting-state functional connectivity and behavior. *NeuroImage* 2019;196:126–141. [PubMed: 30974241]
36. Yeo BTT, Krienen FM, Sepulcre J, et al. The organization of the human cerebral cortex estimated by intrinsic functional connectivity. *J Neurophysiol* 2011;106(3):1125–1165. [PubMed: 21653723]
37. Seabold S, Perktold J. *Statsmodels: Econometric and Statistical Modeling with Python*. PROC. OF THE 9th PYTHON IN SCIENCE CONF 2010;57.
38. Pedregosa F, Varoquaux G, Gramfort A, et al. Scikit-learn: Machine learning in Python. *Journal of Machine Learning Research* 2011;12:2825–2830.
39. Baron RM, Kenny DA. The moderator–mediator variable distinction in social psychological research: Conceptual, strategic, and statistical considerations. *Journal of Personality and Social Psychology* 1986;51(6):1173–1182. [PubMed: 3806354]
40. Hayes AF. *Introduction to Mediation, Moderation, and Conditional Process Analysis, Second Edition: A Regression-Based Approach*. Guilford Publications; 2017.
41. Bolton PF, Clifford M, Tye C, et al. Intellectual abilities in tuberous sclerosis complex: Risk factors and correlates from the Tuberous Sclerosis 2000 Study. *Psychological Medicine* 2015;45(11):2321–2331. [PubMed: 25827976]
42. Doherty C, Goh S, Poussaint TY, et al. Prognostic significance of tuber count and location in tuberous sclerosis complex. *Journal of Child Neurology* 2005;20(10):837–841. [PubMed: 16417883]
43. van Eeghen AM, Pulsifer MB, Merker VL, et al. Understanding relationships between autism, intelligence, and epilepsy: A cross-disorder approach. *Developmental Medicine and Child Neurology* 2013;55(2):146–153. [PubMed: 23205844]
44. Meikle L, Talos DM, Onda H, et al. A mouse model of tuberous sclerosis: Neuronal loss of Tsc1 causes dysplastic and ectopic neurons, reduced myelination, seizure activity, and limited survival. *Journal of Neuroscience* 2007;27(21):5546–5558. [PubMed: 17522300]
45. Lado FA, Moshé SL. Role of subcortical structures in the pathogenesis of infantile spasms: What are possible subcortical mediators? *International Review of Neurobiology* 2002;49:115–140. [PubMed: 12040889]
46. Chugani HT, Ilyas M, Kumar A, et al. Surgical treatment for refractory epileptic spasms: The Detroit series. *Epilepsia* 2015;56(12):1941–1949. [PubMed: 26522016]
47. Jacobs J, Rohr A, Moeller F, et al. Evaluation of epileptogenic networks in children with tuberous sclerosis complex using EEG-fMRI. *Epilepsia* 2008;49(5):816–825. [PubMed: 18177362]
48. Chugani HT, Shewmon DA, Sankar R, et al. Infantile spasms: II. Lenticular nuclei and brain stem activation on positron emission tomography. *Annals of Neurology* 1992;31(2):212–219. [PubMed: 1575460]
49. Wycis HT, Baird HW, Spiegel EA. Long range results following pallidotomy and pallidoamygdalotomy in certain types of convulsive disorders. *Stereotactic and Functional Neurosurgery* 1966;27(1–3):114–120.
50. Uusisaari M, Knöpfel T. GABAergic synaptic communication in the GABAergic and non-GABAergic cells in the deep cerebellar nuclei. *Neuroscience* 2008;156(3):537–549. [PubMed: 18755250]
51. Pearl PL, Vezina LG, Saneto RP, et al. Cerebral MRI abnormalities associated with vigabatrin therapy. *Epilepsia* 2009;50(2):184–194. [PubMed: 18783433]

52. Desguerres I, Marti I, Valayannopoulos V, et al. Transient magnetic resonance diffusion abnormalities in West syndrome: The radiological expression of non-convulsive status epilepticus? *Developmental Medicine and Child Neurology* 2008;50(2):112–116. [PubMed: 18201300]
53. Sutoo D, Akiyama K, Yabe K. Quantitative maps of GABAergic and glutamatergic neuronal systems in the human brain. *Human Brain Mapping* 2000;11(2):93–103. [PubMed: 11061336]
54. Scantlebury MH, Galanopoulou AS, Chudomelova L, et al. A model of symptomatic infantile spasms syndrome. *Neurobiology of Disease* 2010;37(3):604–612. [PubMed: 19945533]
55. Murphy K, Fox MD. Towards a consensus regarding global signal regression for resting state functional connectivity MRI. *NeuroImage* 2017;154:169–173. [PubMed: 27888059]
56. Boes AD, Prasad S, Liu H, et al. Network localization of neurological symptoms from focal brain lesions. *Brain* 2015;138(10):3061–3075. [PubMed: 26264514]
57. Horn A, Reich M, Vorwerk J, et al. Connectivity Predicts deep brain stimulation outcome in Parkinson disease. *Ann Neurol* 2017;82(1):67–78. [PubMed: 28586141]
58. Weigand A, Horn A, Caballero R, et al. Prospective Validation That Subgenual Connectivity Predicts Antidepressant Efficacy of Transcranial Magnetic Stimulation Sites. *Biol Psychiatry* 2018;84(1):28–37. [PubMed: 29274805]
59. Cash RFH, Zalesky A, Thomson RH, et al. Subgenual Functional Connectivity Predicts Antidepressant Treatment Response to Transcranial Magnetic Stimulation: Independent Validation and Evaluation of Personalization. *Biological Psychiatry* 2019;86(2):e5–e7. [PubMed: 30670304]
60. Wang Q, Akram H, Muthuraman M, et al. Normative vs. patient-specific brain connectivity in deep brain stimulation. *NeuroImage* 2021;224:117307. [PubMed: 32861787]
61. Im K, Ahtam B, Haehn D, et al. Altered Structural Brain Networks in Tuberous Sclerosis Complex. *Cerebral Cortex* 2016;26(5):2046–2058. [PubMed: 25750257]
62. Wu JY, Goyal M, Peters JM, et al. Scalp EEG spikes predict impending epilepsy in TSC infants: A longitudinal observational study. *Epilepsia* 2019;60(12):2428–2436. [PubMed: 31691264]
63. Davis PE, Kapur K, Filip-Dhima R, et al. Increased electroencephalography connectivity precedes epileptic spasm onset in infants with tuberous sclerosis complex. *Epilepsia* 2019;60(8):1721–1732. [PubMed: 31297797]
64. Kotulska K, Kwiatkowski DJ, Curatolo P, et al. Prevention of Epilepsy in Infants with Tuberous Sclerosis Complex in the EPISTOP Trial [Internet]. *Ann Neurol* 2020;n/a(n/a)[cited 2020 Dec 2] Available from: <https://onlinelibrary.wiley.com/doi/abs/10.1002/ana.25956>

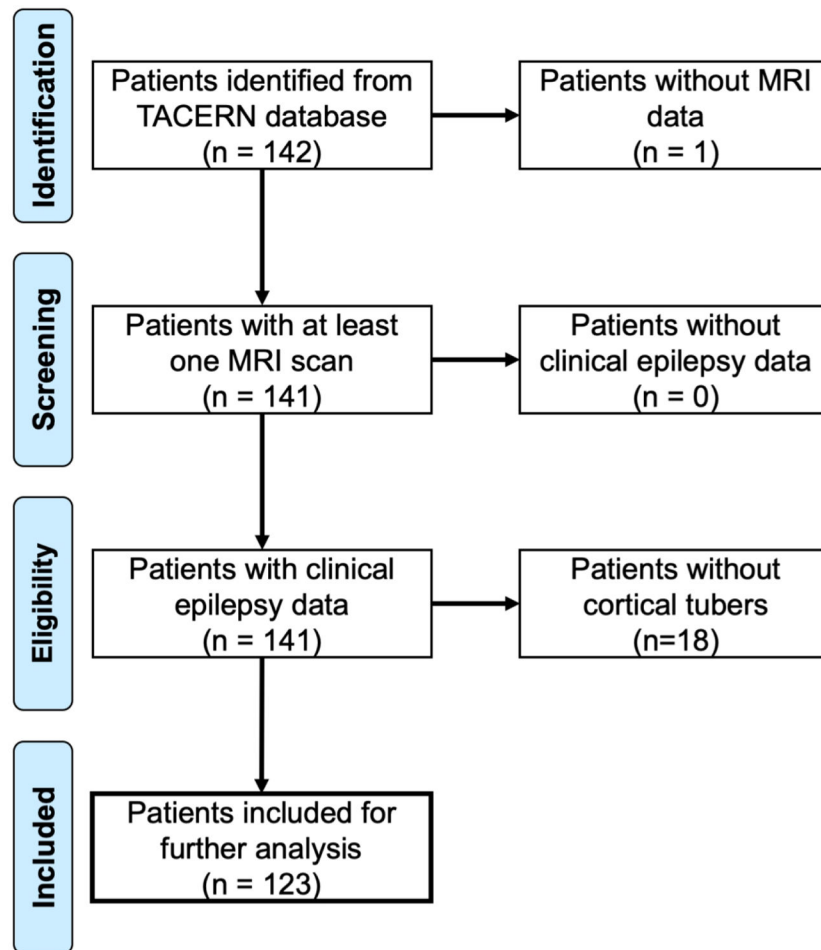


Figure 1: PRISMA Flow Chart identifying TACERN research patients with and without infantile spasms.

Patients were identified from the prospective TACERN cohort study of children with TSC. Inclusion criteria included availability of neuroimaging data of sufficient quality to identify tubers, sufficient clinical follow-up to accurately delineate patients who did or did not develop infantile spasms, and the presence of identifiable tubers on neuroimaging so that tuber locations could be used for lesion network mapping. One hundred and twenty-three patients met these criteria, while 19 were excluded, either due to the lack of available neuroimaging or the absence of detectable tubers.

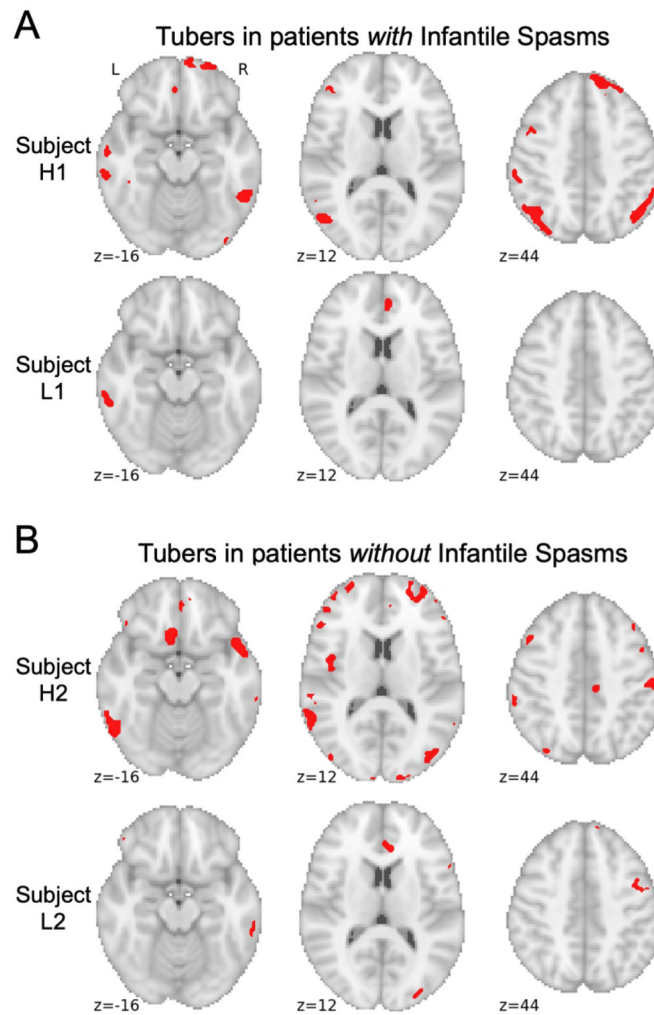


Figure 2 –. Sample tubers distributions from children with and without a history of infantile spasms.

Tubers were segmented from all 123 children using a semi-automated approach and registered to a common brain atlas (MNI 6th gen. atlas). Example tuber distributions are shown in red from the seventy-four children with infantile spasms (A) and the forty-nine children without infantile spasms (B), demonstrating that both groups included children with high tuber burdens (Participants H1 and H2) as well as low tuber burdens (Participants L1 and L2) that could not be visibly distinguished from one another.

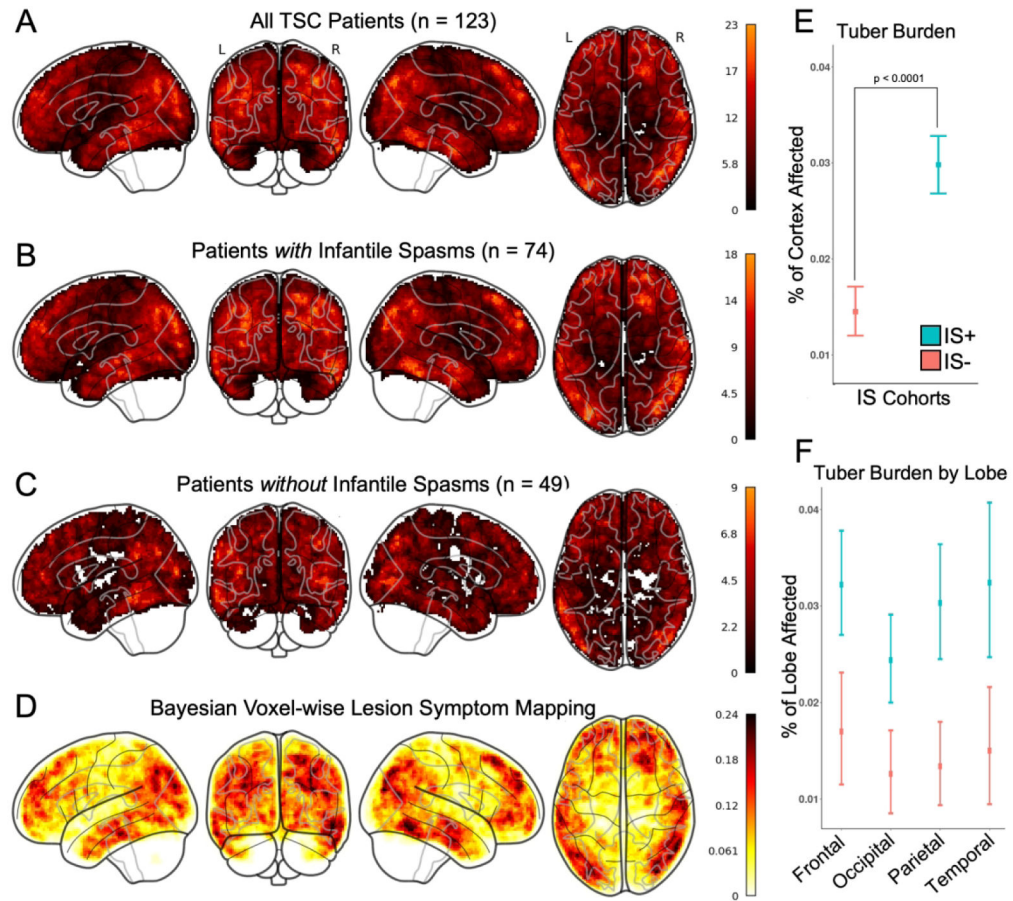


Figure 3 – Increased tuber burden, but not tuber location, is associated with infantile spasms. Binary tuber distribution masks were summed for: all children with TSC (A), the cohort of children with infantile spasms (B), and the cohort of children without infantile spasms (C). Both visual comparison and quantitative spatial analysis (D), did not identify a particular pattern for tuber distribution in general, nor that distinguished between children with and without a history of infantile spasms. While overall tuber burden was statistically different between the two cohorts (E), there was not a statistically significant difference between cortical lobe involvement (F).

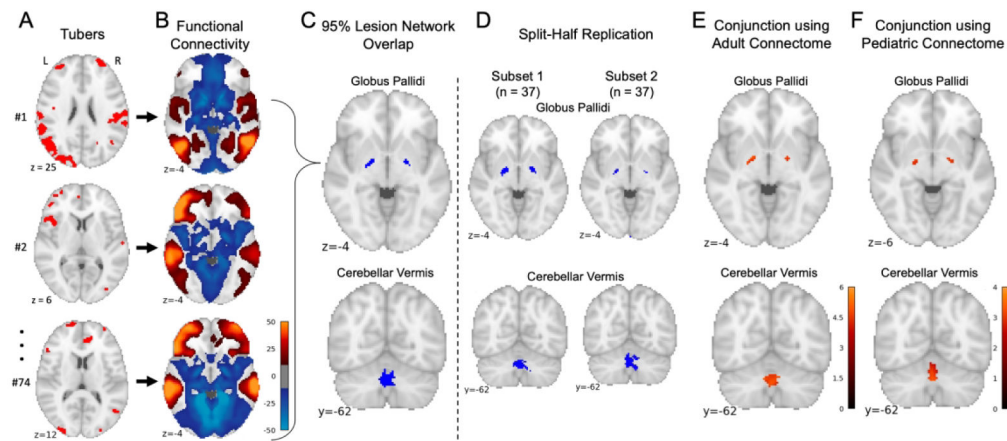


Figure 4 – Lesion network mapping identified three brain regions with consistent negative functional connectivity to tuber distributions associated with infantile spasms.

The 74 tuber distributions associated with infantile spasms were registered to a standardized MNI brain template (A). Brain regions functionally connected to each tuber distribution were identified using a large-scale functional connectivity database of young adult participants (B). Overlap of these functional connectivity maps identified three brain regions connected to >95% of tuber distributions associated with infantile spasms: the left and right globus palladi and the cerebellar vermis (C). Consistent connected regions were also identified in two independent subsets (D). Of note, overlap of functional connectivity maps from the 49 children without infantile spasms did not reveal any consistently connected regions. Regions where connectivity was specific to infantile spasms were then identified by voxel-wise two-sample t-test between children with infantile spasms and those without. The conjunction of a mask of these significant voxels and the lesion network mapping analysis above generated a map of regions both sensitive and specific for infantile spasms, here shown controlling for genetic etiology as a covariate (E). This process was repeated with an alternate large-scale functional connectivity database of 9-year-old participants identifying consistent results (F).

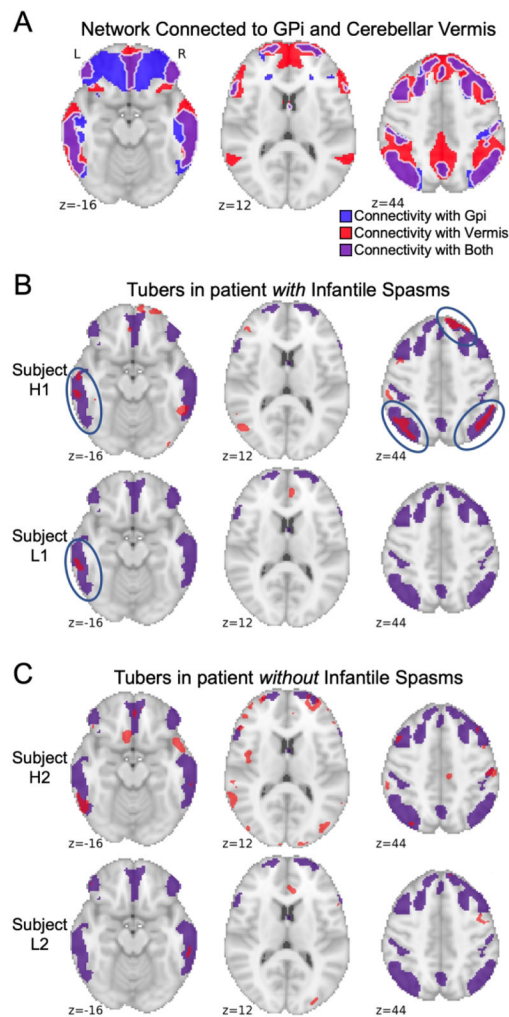


Figure 5 –. Lesion network connectivity with the bilateral globus pallidus and cerebellar vermis predicts locations where tubers are more likely to cause infantile spasms.

The intersection of connectivity with the globus pallidi (Gpi, blue shading) and connectivity with the cerebellar vermis (red shading) defined a specific network of areas (purple shading) predicted to be highly likely to cause infantile spasms if lesioned (A). As a demonstration, the same four patients shown in Figure 2, two with infantile spasms and two without infantile spasms, and with either high or low tuber burden, are again shown here with tuber burden (in red) compared to the identified network (in purple) (B and C). Among patients with infantile spasms (B), it can be seen that tubers are more likely to overlap with the predicted network (blue circles). Conversely, among patients without infantile spasms (C), tubers largely do not overlap with the predicted network.

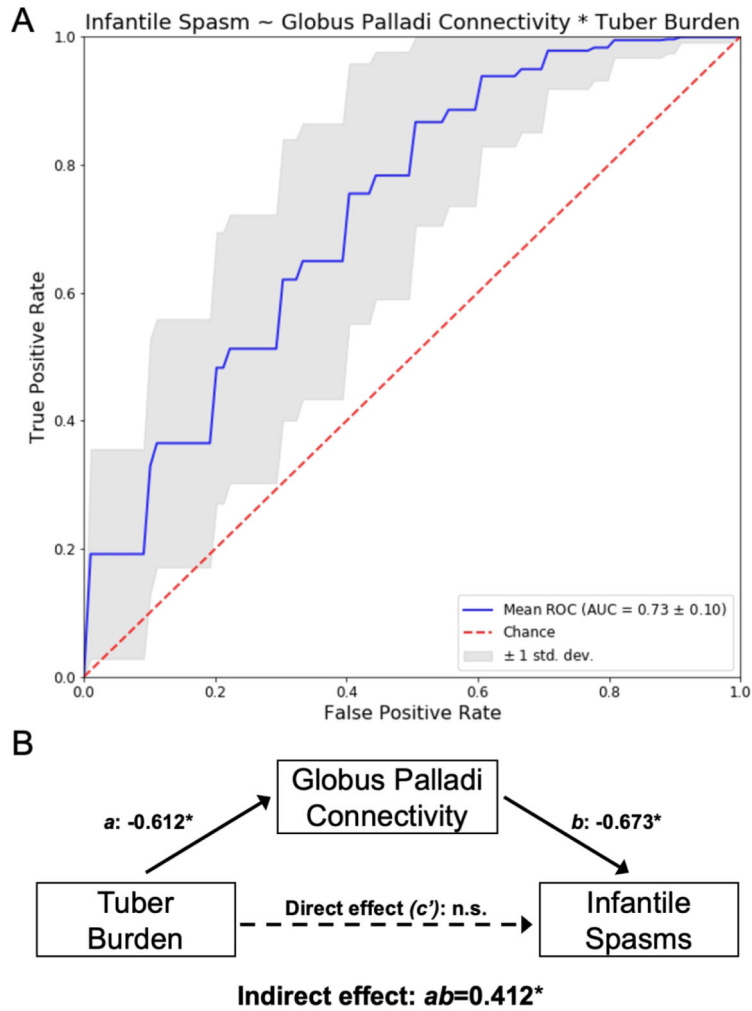


Figure 6 –. Logistic regression and statistical mediation analyses finds that globus pallidus connectivity is a stronger predictor of infantile spasms than tuber burden and may mediate the observation that increased tuber burden is associated with infantile spasms.

The performance of predicting infantile spasms from patients’ tuber burden and globus pallidus connectivity (Table 2, Model 5) was assessed using repeated stratified k-fold cross validation. First, the 123 TSC patients were divided into five groups, then a logistic model was trained using four of these groups, e.g., 80% of the data, and tested for accuracy on the remaining hold-out group, e.g., 20% of the data. The classification results of 5,000 iterations of this process, with random shuffling within groups, was used to create Receiver Operating Characteristic (ROC) curves (A). The mean ROC curve for this model is shown here (blue), along with a one standard deviation cloud (grey) compared to chance (red). The Area Under the Curve (AUC) was also calculated to be 0.73 (standard deviation = 0.10). A separate statistical mediation analysis (B) identified that the relationship between tuber burden and infantile spasms (path c) is fully mediated by the serial relationship of tuber burden and globus palladi connectivity (path a) and globus palladi connectivity and infantile spasms (path b), with an indirect effect of $ab=0.412$, 95% CI (0.114,0.872). When this mediation is taken into account, tuber burden itself no longer independently predicts (*path c*) infantile

spasms. Importantly, the reverse model found no mediation, i.e., tuber burden does not mediate the relationship between globus pallidus connectivity and infantile spasms.

Author Manuscript

Author Manuscript

Author Manuscript

Author Manuscript

Table 1:

Patient demographics and tuber distribution

	Spasms+	Spasms–	Total
Patients, n	74	49	123
Male sex, n (%)	35 (47)	28 (57)	63 (51)
Mean age at scan, years (range)	2.74 (0.76-5.44)	2.53 (0.32-3.89)	2.66 (0.32-5.44)
Mean age at spasm onset, days (range)	168 (0-519)	n/a	n/a
Genotype, n (% of total)			
<i>TSC1</i> mutation	4 (27.7)	11 (73.3)	15 (100)
<i>TSC2</i> mutation	47 (61.8)	29 (38.2)	76 (100)
No mutation identified	7 (58.3)	5 (41.7)	12 (100)
Unknown	16 (80.0)	4 (20.0)	20 (100)
Median tuber burden, % (25-75% range)			
All cortical grey matter	2.59 (1.58-4.73)	0.85 (0.08-2.34)	2.10 (0.69-3.76)
Frontal Lobe	2.91 (1.50-4.78)	1.04 (0.06-2.66)	2.17 (0.71-4.48)
Parietal Lobe	2.31 (1.33-4.17)	0.95 (0.05-2.76)	1.68 (0.29-3.33)
Temporal Lobe	1.99 (0.87-5.35)	0.42 (0.04-2.32)	1.44 (0.19-3.89)
Occipital Lobe	1.90 (0.87-3.55)	0.88 (0.00-2.03)	1.54 (0.24-2.99)
Tuber frequency, %			
Frontal Lobe	92	59	79
Parietal Lobe	85	53	72
Temporal Lobe	81	47	67
Occipital Lobe	84	53	72

Table 2:

Family of logistic regression models identifying globus pallidus connectivity as the independent variable most predictive of infantile spasms

	Model 1	Model 2	Model 3	Model 4	Model 5	Model 6
Tuber Volume						
OR (95% CI)	2.69 (1.60-4.50)	—	—	—	1.65 (0.90-3.04)	1.67 (0.88-3.15)
<i>p</i>	0.00017	—	—	—	0.11	0.12
Connectivity to the Globus Pallidus						
OR (95% CI)	—	2.68 (1.66-4.33)	—	2.37 (1.08-5.23)	1.96 (1.10-3.50)	2.21 (1.00-4.87)
<i>p</i>	—	0.000057	—	0.032	0.023	0.04978
Connectivity to the Cerebellar Vermis						
OR (95% CI)	—	—	2.27 (1.48-3.49)	1.15 (0.55-2.42)	—	0.95 (0.44-2.08)
<i>p</i>	—	—	0.00019	0.71	—	0.91
AIC	150.84	147.83	152.63	149.69	146.98	148.96
pseudo R-squared	0.112	0.130	0.101	0.131	0.148	0.148

OR = Odds Ratio, CI = Confidence Interval, AIC = Akaike Information Criterion